Chemistry
A European
Journal

Chemistry Europe
European Chemical Societies Publishing

Accepted Article

Title: Ruthenium(II) polypyridyl complexes with benzoxazole derivatives and non-innocent ligands as effective antioxidants in human neuroblasts

Authors: Gina Elena Giacomazzo, Luca Conti, Daniele Paderni, Patrick Severin Sfragano, Lorenzo Quadrini, Eleonora Macedi, Camilla Andreini, Chiara Donati, Caterina Bernacchioni, Gloria Mulas, Barbara Valtancoli, Ilaria Palchetti, Luca Giorgi, Vieri Fusi, Francesca Cencetti, and Claudia Giorgi

To be cited as: *Chem. Eur. J.* **2024**, e202400834

Link to VoR: https://doi.org/10.1002/chem.202400834

WILEY VCH

10.1002/chem.202400834

RESEARCH ARTICLE

RUTHENIUM(II) POLYPYRIDYL COMPLEXES WITH BENZOXAZOLE DERIVATIVES AND NON-INNOCENT LIGANDS AS EFFECTIVE ANTIOXIDANTS IN HUMAN NEUROBLASTS

Gina Elena Giacomazzo,[a] Luca Conti,*[a] Daniele Paderni,[b] Patrick Severin Sfragano,[a] Lorenzo Quadrini,[a] Eleonora Macedi,[b] Camilla Andreini,[c] Chiara Donati,[d] Caterina Bernacchioni,[d] Gloria Mulas,[d] Barbara Valtancoli,[a] Ilaria Palchetti,[a] Luca Giorgi,[b] Vieri Fusi,[b] Francesca Cencetti,*[d] Claudia Giorgi.*[a]

[a] G. E. Giacomazzo PhD, P. S. Sfragano PhD, L. Quadrini, Prof. I. Palchetti, Prof. B. Valtancoli, L. Conti PhD, Prof. C. Giorgi
Department of Chemistry "*Ugo Schiff*"
University of Florence
via della Lastruccia 3, 50019, Sesto Fiorentino (FI), Italy.
E-mail: luca.conti@unifi.it, claudia.giorgi@unifi.it

[b] D. Paderni PhD, Prof. L. Giorgi, Prof. V. Fusi
Department of Pure and Applied Sciences "*Carlo Bo*"
University of Urbino
Via della Stazione 4, 61029, Urbino. Italy.

[c] Dr. C. Andreini
Istituto Nazionale di Genetica Molecolare-INGM
Via Francesco Sforza 35, 20122, Milano, Italy.

[d] Prof. F. Cencetti, Prof. C. Donati, Prof. C. Bernacchioni, Dr. G. Mulas
Department of Experimental and Clinical Biomedical Sciences "*Mario Serio*"
University of Florence
Viale Morgagni, 50, 50134, Florence, Italy.
E-mail: francesca.cencetti@unifi.it

Supporting information for this article is given via a link at the end of the document.

Abstract: Ruthenium(II) polypyridyl complexes continue to raise increasing interest for the encouraging results in several biomedical areas. Considering their vast chemical-physical repertoire, in particular the possibility to switch from the sensitization of reactive oxygen species (ROS) to ROS-scavenging abilities by tuning the nature of their ligands, it is therefore surprising that their potential as antioxidants has not been largely investigated so far. Herein, we explored the antioxidant behaviour of the novel ruthenium compound [Ru(dbpy)(2,3-DAN)Cl]PF_6 (**Ru1**), featuring a benzoxazole derivative (dpby = 2,6-bis(4-methyl-2-benzoxazolyl)pyridine) and the non-innocent 2,3-diamminonaftalene (2,3-DAN) ligand, along with the reference tpy-containing analogue [Ru(tpy)(2,3-DAN)Cl]PF_6 (**Ru2**) (tpy = 2,2':6',2''-terpyridine). Following the synthesis and the electrochemical characterization, chemical antioxidant assays highlighted the beneficial role of dpby for the ROS-scavenging properties of **Ru1**. These data have been corroborated by the highest protective effect of **Ru1** against the oxidative stress induced in SH-SY5Y human neuroblastoma, which exerts pro-survival and anti-inflammatory actions. The results herein reported highlight the potential of **Ru1** as pharmacological tool in neurodegenerative diseases and specially prove that the antioxidant properties of such compounds are likely the result of a non-trivial synergetic action involving the bioactive ligands in their chemical architectures.

Introduction

It is widely accepted that neural tissue possesses a high lipid content and consumes a huge quantity of oxygen that may result in an excess of reactive oxygen species (ROS) generation, making it vulnerable to oxidative stress. In particular, neuronal membranes have been shown to have a high amount of polyunsaturated fatty acids that are extremely sensible to ROS.[1] Given that low levels of ROS are required for normal cellular signalling, exogenous or endogenous increase in ROS amount is promptly regulated and rebalanced. When the adaptive systems are compromised or the ROS production increases excessively over time, it creates a state of oxidative stress where ROS induce damage to cellular macromolecules such as DNA, lipids, and proteins, ultimately leading to necrosis and apoptotic cell death. Oxidative stress is one of the risk factors for the development and progression of chronic neurological diseases such as Parkinson's disease (PD), Alzheimer's disease (AD), Huntington's disease (HD), and amyotrophic lateral sclerosis (ALS).[2]

Under normal conditions, almost 0.2%-2% of the electrons that flow through the mitochondrial transport chain leaks to partially reduce the molecular O_2 that generates ROS.[3] When the mitochondrial respiratory chain is disrupted by chemical components (respiratory inhibitors) or mutations in mitochondrial genes that encode respiratory enzymes, ROS generation and accumulation increase.[4] The most important ROS are superoxide anion ($O_2^{\cdot-}$), hydroxyl radical ($^{\cdot}OH$), hydrogen peroxide (H_2O_2) and singlet oxygen ($^1O_2$). ROS subtract an electron to the surrounding biomolecules that become reactive species spreading the oxidation in the near environment. Antioxidants are stable compounds that can interrupt this propagational chain by donating an electron to the pro-oxidant molecule, preventing damage from oxidative stress. Antioxidants are classified based on their mechanism of action: some enzymes catalyse the breakdown of the superoxide anion (Superoxide dismutases, SODs) or hydrogen peroxide (Catalases), while there are compounds that donate hydrogen to peroxide radicals. The potency of natural antioxidants, such as vitamins, polyphenols and carotenoids (just to name a few), is typically not enough to counteract the escalation of oxidative stress, thus making it of paramount importance the research of novel and effective compounds. Therapeutic approaches aimed at reducing oxidative stress could be a valid strategy to counteract the clinical evolution of associated pathologies such as neurological diseases. In this scenario, beyond their prospective use as anticancer drugs, ruthenium complexes have demonstrated encouraging results as neuroprotective drugs in the field of neurology.[5,6] For instance, in

10.1002/chem.202400834

RESEARCH ARTICLE

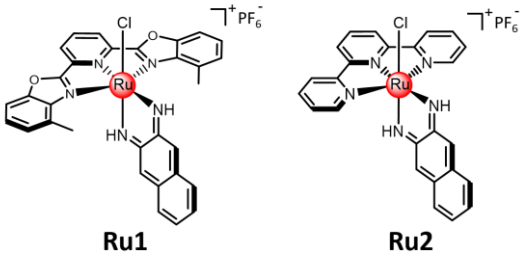

Scheme 1. Ruthenium complexes **Ru1** and **Ru2** of this study.

the brain of chronic induced-cerebral hypoperfusion Swiss mice, Ruthenium red (RR) treatment was shown to decrease thiobarbituric acid levels, increase glutathione levels, and restore superoxide dismutase levels and the activity of its reduced isoform. A reduction of acetylcholinesterase activity, perhaps maintaining cholinergic activity, was also demonstrated.[7] The antioxidant properties of Ruthenium compounds are associated with their ability to be employed as diagnostic tools for neurodegenerative diseases, based on their capability of preventing the aggregation of Aβ peptides generated in the early stages of Alzheimer disease.[8] Of particular interest are ruthenium(II) polypyridyl complexes (RPCs), whose rich chemical-physical repertoire, which includes the capacity to interact with important biological targets, such as DNA and/or proteins, and versatile chemical-physical and photo-physical properties, has made their use promising in various biomedical areas, spanning from the research of novel anticancer[9,10] to antibacterial agents.[11,12] Their popularity has been recently associated to the use in the so-called photodynamic therapy,[13-16] an emerging therapeutic approach that has led to the first RPC to complete phase Ib trial for the treatment of non-muscle invasive bladder cancer, the McFarland compound TLD 1433,[17] but the use of RPCs in the complementary photoactivated chemotherapy technique has been also well described.[18-21]

Particularly intriguing is the possibility to optimally tune the overall chemical-physical properties of RPCs by finely choosing the nature of ligands in their octahedral geometries, making it possible, for instance, to switch from a compound able to sensitize the ROS formation to one exhibiting ROS scavenging capabilities. This, along with the potential demonstrated by this class of compounds in various biomedical fields, makes it therefore surprising that their role as antioxidant agents has been only poorly considered so far.

Jiang et al. reported on the hydroxyl radical scavenging activity of their complexes $Ru(phen)_2(adppz)](ClO_4)_2$ and $[Ru(dip)_2(adppz)](ClO_4)_2$ (adppz = dipyrido[3,2-*a*:2′,3′-*c*]phenazine, dip = 4,7-diphenyl-1,10-phenanthroline, phen = 1,10-phenanth),[22] similarly to what previously described by Huang et. al for their $[Ru(dmb)_2(maip)](ClO_4)_2$ complex (dmb = 4,4′-dimethyl-2,2′-bipyridine, maip = 2-(3-aminophenyl)imizado[4,5-f][1,10]phenanthroline). A few ligands with well-established antioxidant properties, such as flavonoids or non-steroidal anti-inflammatory drug (NSAIDs), have been inserted into the octahedral geometries of RPCs as well.[23,24] However, despite accumulating evidence, additional research is needed to dissect the potential of RPCs as antioxidant compounds.

Prompted by this scenario, herein we report on a novel ruthenium compound, $[Ru(dbpy)(2,3\text{-}DAN)Cl]PF_6$ (**Ru1**), where a new benzoxazole derivative (dpby = 2,6-bis(4-methyl-2-benzossazolyl)pyridine) and 2,3-diamminonaftalene (2,3-DAN) were respectively inserted in view of the wide spectrum of pharmacological activities associated to benzoxazoles, including antioxidant capacities,[25] and the well-known redox-active properties of the non-innocent, 2,3-DAN chelate.[26] Regarding this latter ligand, it is also important to mention that despite the high redox activity, its direct use as potential antioxidant agent should be avoided in consideration of the toxicity issues commonly associated to primary aromatic amines (PAAs).[27] In this view, the insertion of this ligand into non-toxic ruthenium complexes may provide an appealing strategy to take advantage from the properties conferred by such chelate. A chloride ligand then completes the coordinative requirements of the Ru(II) center (Scheme 1). The reference compound $[Ru(tpy)(2,3\text{-}DAN)Cl]PF_6$ (**Ru2**), with a tpy (tpy = 2,2':6',2''-terpyridine) replacing dbpy, was also considered in this study for comparison. Following the synthesis, the characterization of their electrochemical and cell-free antioxidant behaviour, the protective effects of **Ru1** and **Ru2** were evaluated against the cellular damage induced by pro-oxidant species in SH-SY5Y neuroblastoma cell line, by putting a special emphasis on the involved molecular mechanisms responsible for the observed biological effects.

The aim of this work is to highlight the perspectives arising from the use of RPCs as antioxidants, beyond to demonstrate that their biological behavior may result from a non-trivial modulation of the bioactivities of ligands combined in their chemical architectures.

Results and Discussion

Synthesis, characterization, and stability of ruthenium complexes. The tridentate dpby ligand was synthesized by the condensation of pyridine-2,6-dicarboxylic acid (**2**), previously obtained by oxidation from the commercially available 2,6-dimethyl pyridine,[28] with two equivalents of 2-amino-3-methylphenol (**1**) in polyphosphoric acid (PPA) at 160 °C,[29,30] as shown in Scheme 2 (panel a).

The synthesis of ruthenium complexes **Ru1** and **Ru2** has been performed by adopting the synthetic routes reported in panels b of Scheme 2. Briefly, these complexes were obtained through the preliminary preparation of their neutral Ru(III) precursors $Ru(L)Cl_3$ (L = dpby or tpy), which was accomplished by reaction of the tridentate ligands with equimolar amounts of $RuCl_3{\cdot}3H_2O$ in 1,4-dioxane ($Ru(dpby)Cl_3$) or ethanol ($Ru(tpy)Cl_3$) under reflux (*step I*). Then, in the following step (*step II*), these intermediates were allowed to react with the 2,3-diaminonapthalene (2,3-DAN) in ethanol in the presence of TEA as a base, and precipitated with aqueous KPF_6 affording the final hexafluorophosphate salts **Ru1** and **Ru2** in yields respectively of 84 and 32%. The identity of compounds was established through ^1H, ^{13}C, COSY and HSQC NMR spectroscopy, UV-Vis absorption spectroscopy, mass spectrometry (MS) and infrared spectroscopy (IR) (Fig. S1-S14, SI).

Attempts to synthesize the Ru(III) precursor of **Ru1**, $Ru(dpby)Cl_3$, by using ethanol, namely the standard solvent employed in the preparation of $Ru(L)Cl_3$ compounds with L = tpy,[31] or the nitrogen analogue of dpby 2,6-*bis*(benzimidazol-2-yl)pyridine (bbp),[32] were also made but, contrary to 1,4-dioxane, turned out to be unsuccessful. This indicates a difference in reactivity between dpby and other nitrogen-containing analogues, associable to the two benzoxazole moieties in the new tridentate ligand. In this respect, the observed effect of the solvent in *step I* for the preparation of $Ru(dpby)Cl_3$ could be tentatively rationalized by considering the stabilization of the metal-uncoordinated form of ligand by the protic molecules of ethanol, preventing the dpby chelation to the electron-poor Ru(III) center. In case of the aprotic 1,4-dioxane, this stabilization would be less efficient, preserving a sufficient coordination ability of the dpby nitrogen donors to form the corresponding Ru(III) complex. This would be also supported by the earlier reported use of 1,4-dioxane to allow the Ru(III) coordination by the sulphur-containing analogue 2,6-*bis*-(2-benzothiazolyl)pyridine tridentate ligand.[33]

In the final ruthenium complexes, it can be highlighted the iminic nature (*i.e.* diimine) of the chelating nqdi ligands, which can be associated to the oxidation of the redox-active 2,3-DAN ligand to its nqdi imine species (see Scheme 2, panel c) accompanying the

10.1002/chem.202400834

RESEARCH ARTICLE

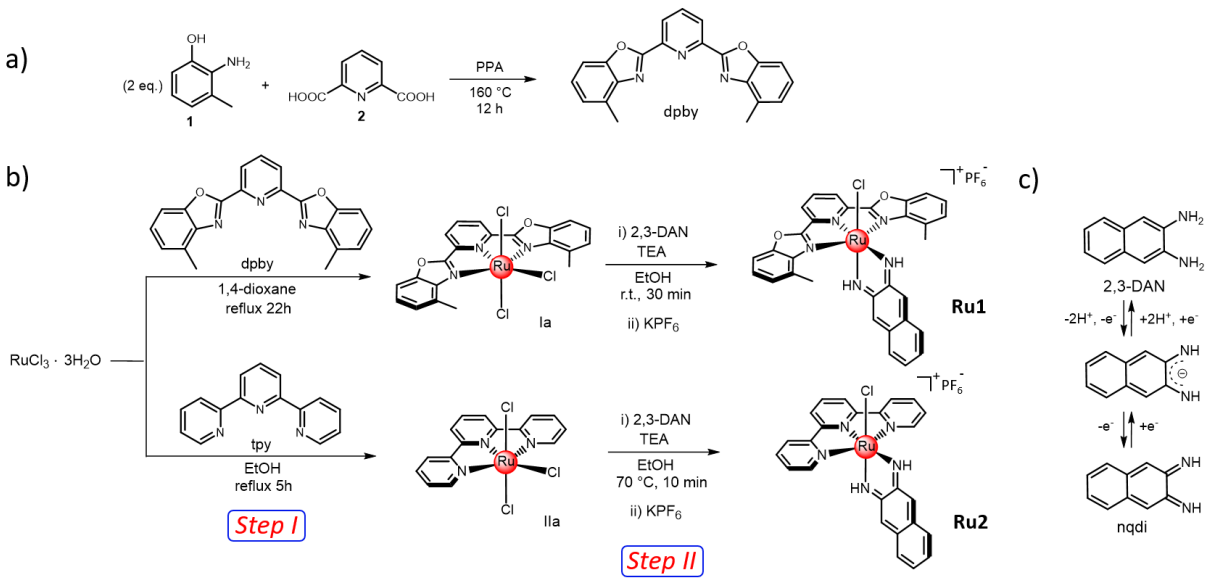

Scheme 2. Schematic representation of the synthetic routes followed for the synthesis of the tridentate dpby ligand (a) and of ruthenium complexes **Ru1** and **Ru2** (b). On the right are schematized the redox equilibria involving 2,3-diaminonaphthalene (2,3-DAN) and its oxidized form, the 2,3-naphthoquinone diimine (nqdi)(c).

reduction of Ru(III) centers to Ru(II) during the last reaction step. This coordination mode, which is in agreement with what generally reported for analogues ruthenium complexes with non-innocent ligands prepared under similar experimental conditions,[33,34-36] has been confirmed by NMR and MS analysis. In fact, the positive-ion electrospray mass (ESI MS) spectra of **Ru1** displays the isotopic pattern of the mono positively charged species $[Ru(dpby)(nqdi)Cl]^+$, centered at 634.5 (m/z = 1) (Figures S8-9, SI), whereas the two peaks at considerably high frequencies (13.78 and 12.22 ppm, each integrating 1H), in the ^{1}H NMR spectrum of **Ru1** (Figure S4, SI) are typically attributable to imine protons.[26,35] Similar evidences have been recently reported for the reference compound **Ru2**.[26]

In Figure 1 are shown the electronic absorption spectra of **Ru1** and **Ru2** collected in acetonitrile whereas a comparison between the molar absorption coefficients at different absorption maxima measured in acetonitrile and water is reported in Table 1; the absorption spectra collected in water are instead reported in Fig. S14 (SI).

As shown, both compounds display the typical absorption profiles of ruthenium polypyridyl complexes, characterized by intense bands in the 250-330 nm range, that can be attributed to intra-ligand π→π* transitions of polydentate ligands, plus a broad absorption in the visible region, attributable to the metal-to-ligand dπ(Ru)→π*(polypyridyl ligands) charge transfer (MLCT) transitions, with maxima at 540 nm (ε = 19.7 x 10^3 M^{-1} cm^{-1}) and 520 nm (ε = 23.5 x 10^3 M^{-1} cm^{-1}) for **Ru1** and **Ru2**, respectively. It can be noted that the presence of the dpby ligand in **Ru1** is responsible for a considerably red-shift of the MLCT absorption maxima, of *ca.* 710 cm^{-1}, compared to **Ru2**, attributable to the augmented π-extension of dpby relative to tpy. A similar effect is also displayed by the two compounds in water (670 cm^{-1}) (Fig. S14, SI). On the other hand, both complexes turned out to be scarcely emissive (data not shown), in line with the notoriously scarce luminescent properties of tridendate-containing RPCs.[37,38]

Lastly, the stability of the two metal complexes in water at pH 7 was checked by monitoring their UV-vis absorption spectra over a total period of 24 hours (Fig. S15, SI). Slight (**Ru2**) to sharper (**Ru1**) decreases in intensity and hypsochromic shifts of the MLCT band of complexes were observed indicating, in analogy to previous studies,[26,39] the possible hydrolysis of the Ru(II)-bound chloride ion at the higher time frames investigated.

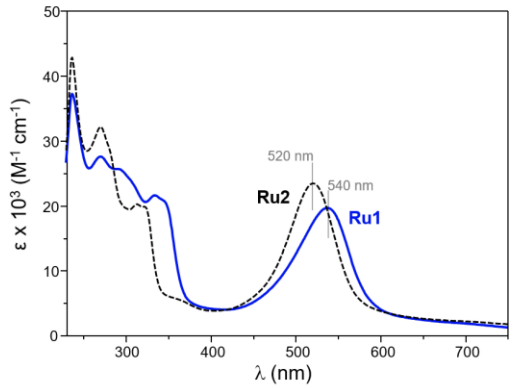

Figure 1. Electronic absorption spectra of ruthenium complexes **Ru1** and **Ru2** registered in acetonitrile.

Table 1. Electronic absorption maxima measured in acetonitrile and water.

Complex	λ_{abs}/nm (ε x 10^3 M^{-1} cm^{-1}) in CH_3CN	λ_{abs}/nm (ε x 10^3 M^{-1} cm^{-1}) in H_2O
Ru1	236 (37.2), 269 (27.6), 291 (25.7), 334 (21.6), 540 (19.7)	236 (37.6), 264 (24.2), 293 (21.8), 335 (21.8), 529 (18.1)
Ru2	236 (42.9), 270 (32.2), 317 (20.0), 520 (23.5)	230 (42.5), 270 (28.8), 313 (21.3), 511 (21.1)

Antioxidant activity of ruthenium compounds. The presence of redox-active moieties in the chemical architectures of ruthenium complexes prompted us to investigate their redox behaviour and antioxidant activity, prior to test their *in-cell* biological potential.

The redox properties of the two ruthenium compounds were first analysed through cyclic voltammetry (CV) measurements (see experimental section for further details), along with the uncoordinated 2,3-DAN and the tridendate tpy and dpby ligands for comparison. As shown in Figure 2a, in the CV scans from -0.5 to +2.5 V of 2,3-DAN are present two broad anodic peaks, respectively centered at around +0.360 V and +0.830 V, in line with the electrochemical behavior known for 2,3-DAN.[40] Electroactivity in this range of potential is also evident in the CV

10.1002/chem.202400834
WILEY VCH

RESEARCH ARTICLE

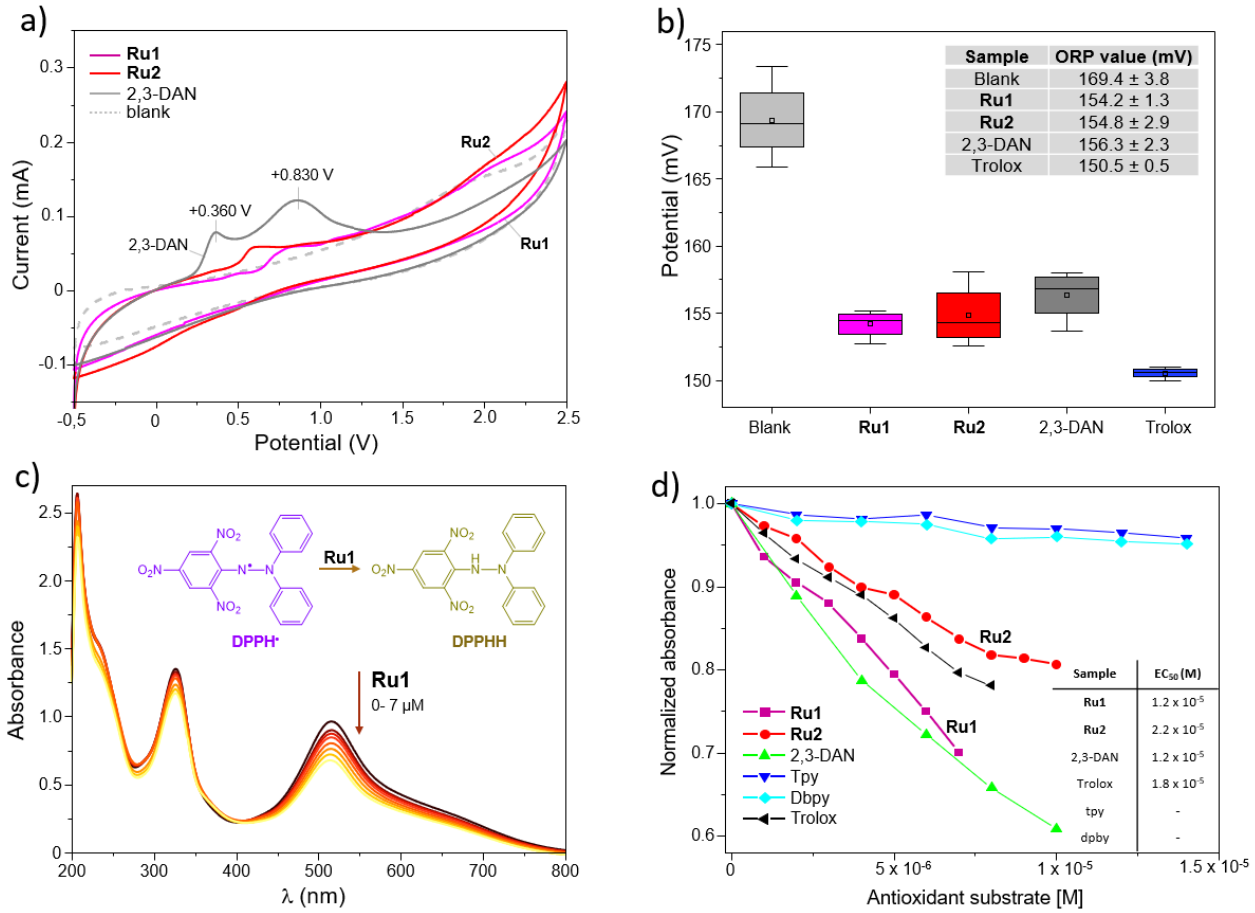

Figure 2. a) CV analysis of ruthenium complexes and 2,3-DAN (1 mM in acetonitrile with 0.1 M Bu_4NClO_4 as a non-complexing supporting electrolyte, scan rate 25 mV/s). The solutions of tested compounds were poured into a cell with a three-electrode setup; a Glassy Carbon working electrode (Ø 5 mm), a Pt counter electrode, and an external Acetonitrile Ag/$AgNO_3$ reference electrode filled with 0.1 M $AgNO_3$. b) ORP measurements for 4 mL of 50 μM of ruthenium complexes, 2,3-DAN, and 50 mM Trolox in 10 mM phosphate buffer at pH 7, 250 mM acetonitrile. c) UV-Visible absorption spectra of DPPH in methanol (75 μM, 2mL) in the presence of increasing concentrations of **Ru1**. d) Normalized absorbance values of DPPH• at 516 nm as a function of substrate's concentration.

scans of both ruthenium complexes **Ru1** and **Ru2**, as denoted by the wide oxidation shoulder displayed by these compounds in the potential window covered by the abovementioned peaks of 2,3-DAN. No peculiar peaks in the investigated potential range were instead found for dpby and tpy. This would indicate that the electroactivity of 2,3-DAN is somehow preserved in the two ruthenium complexes, albeit with different extents as denoted by the slight differences present in their CV profiles.

The contribution by the non-innocent 2,3-DAN in the redox properties of both ruthenium complexes was further confirmed by measurements of the oxidation-reduction potential (ORP). ORP is indeed an important physicochemical parameter that can give useful information about the oxidative or reductive properties of a tested solution. ORP measurements of ruthenium complexes were performed as described in the experimental section and compared with that of 2,3-DAN and Trolox, the latter being an analogue of Vitamin E standardly used as reference for the antioxidant activity;[41] the obtained results are shown in Figure 2b, whereas the corresponding values are listed in the inset on top-right of the figure. As shown, **Ru1** and **Ru2** display similar ORP values, of 154.2 ± 1.3 mV and 154.8 ± 2.9 mV respectively, that also turn out to be close to that of 2,3-DAN, of 156.3 ± 1.3 mV.

The antioxidant activity of ruthenium complexes was then inspected by exploiting the DPPH• (DPPH• = α,α-diphenyl-β-picrylhydrazyl radical) scavenger activity assay,[42,43] a standard procedure to evaluate the antioxidant behaviour of a given substrate based on the monitoring of the decrease of the UV-Vis absorbance of DPPH• in the presence of a candidate antioxidant. In particular, the spare electron on the stable free radical DPPH• is responsible for its deep violet colour, characterized by an intense absorption band centered at 516 nm in methanolic solution. In the presence of a substance capable of donating a hydrogen radical, or an electron, DPPH• gives rise to its stable, diamagnetic, hydrazine form (DPPH-H), resulting in a colour change from purple to yellow, associated with the decrease of the absorption at 516 nm. Therefore, the variation of this band can be taken as diagnostic of the potential DPPH•-scavenging activity of a given substrate.

In Figure 2c are shown the UV-Vis spectra of a methanolic solution of DPPH• collected in presence of increasing concentrations of **Ru1**; the corresponding titrations for **Ru2**, the free ligands 2,3-DAN, dpby, tpy and of Trolox taken as positive control, are reported in SI, Fig. S16.

As shown, the strong absorption of DPPH• at 516 nm undergoes a marked and progressive hypochromism in the presence of increasing concentrations of **Ru1**, indicating a high activity of this compound towards the neutralization of DPPH radical. A similar, but less intense, effect was also displayed by **Ru2** (Fig. S15a), whereas, and in agreement with the electrochemical analysis, among the free tridentate ligands and 2,3-DAN, only the latter one exhibited a significant effect, being comparable to that of **Ru1** (Fig. S15b). These results can be better appreciated by comparing their %DPPH• scavenging activity and EC_{50} values (Figures 2d and S17 of SI), the latter ones referring to the substrate concentration that reduces by half the purple colour of DPPH• and reckoned as described in the experimental section. From these data, **Ru1** and 2,3-DAN emerged to possess the highest antioxidant properties, being superior to that of Trolox

10.1002/chem.202400834

(EC_{50}(Trolox) = 18 μM), with EC_{50} values of 12 μM. It is significant to mention that the antioxidant behaviour of **Ru1** is also superior to the ones of other documented ruthenium complexes (EC_{50} values ranging between 24 and 59.7 μM).[44,45] **Ru2** was found to be associated to an EC_{50} value of 22 μM, comparable to that of Trolox.

To further inspect a possible role of the tridentate ligands based on their electronic nature, Natural Bond Orbital (NBO) analysis was carried out. From these studies, which were performed on the two complexed cations $[dbpy\text{-}Ru]^{2+}$ and $[tpy\text{-}Ru]^{2+}$ (see SI for a detailed description), it emerged a charge of +0.7636e at the Ru center in $[dbpy\text{-}Ru]^{2+}$, namely lower by 0.2902e if compared to that of $[tpy\text{-}Ru]^{2+}$. This highlighted a major electron-donor character of dbpy in **Ru1** relative to the one of tpy in **Ru2** and therefore, might explain the differences emerged in the antioxidant behavior displayed by the two compounds. In other words, this suggests that the different electronic nature of the tridentate ligands may variously modulate the electroactive properties conferred by the redox-active 2,3-DAN chelate.

Lastly, beside the analysis of the ability of ruthenium complexes to act as scavengers of ROS, their eventual capability to sensitize the ROS formation was also considered. This was investigated employing 1,5-dihydroxynaphthalene (DHN) as an indirect singlet oxygen reporter and by monitoring the eventual ROS sensitization from acetonitrile solutions of ruthenium complexes subjected to different irradiation time frames (LED light, λ > 430 nm, 30 W). As shown in Figure S18 (SI), no appreciable Juglone formation, the photooxidation product of DHN, was observed upon DHN irradiation in the presence of ruthenium complexes, thus confirming the scarce photosensitization by these compounds. This is in line with what generally reported for tridentate-containing RPCs, and, along with the poor luminescent features (*vide supra*), could be ascribed to the efficient thermal population of the ^{3}MC states and subsequent rapid nonradiative decay typically associated to this class of compounds.[37]

Antioxidant effect of Ru1 and Ru2 in human neuroblasts

The specific aim of this study was to evaluate and compare the protective effect of ruthenium complexes **Ru1** and **Ru2** on the induced cellular damage in SH-SY5Y neuroblastoma cell line. As pro-oxidant species able to increase oxidative stress in cells we used hydrogen peroxide, H_2O_2, that promote cellular oxidative damage in several experimental models of neurodegenerative processes,[46] Cisplatin (CDDP), a chemotherapeutic drug that induces neurotoxicity, as well as Lipopolysaccharides (LPS), a component of the outer membrane of Gram-negative bacteria. In both glial cells and neurons LPS leads to the production of inflammatory cytokines like TNFα, IL-1β and IL-6.[47]

Prior to investigate the protective effect of ruthenium complexes, their uptake by SH-SY5Y cells was investigated through inductively coupled plasma atomic emission spectrometry (ICP-AES) at different dosages (1-10 μM) and employing different incubation times (6-24 h); the obtained results are reported in Figure 3. As shown, the uptake of metal complexes was already visible at 6 hours treatment at both concentrations, and it became higher at 10 μM concentration after 24 hours. It can be also noted that, while the cellular uptake of the two complexes was substantially the same when dosed at 1 μM, considerable differences emerged at 10 μM. In particular, upon 24 hours incubation the internalization of **Ru1** turned out to be almost two times higher than that of **Ru2**, thus proving that, beyond the *cell-free* antioxidant behavior, the presence of the dpby tridentate ligand in the chemical architecture of this complex has a positive effect also on its capacity to be internalized by SH-SY5Y cells. For these reasons, we decided to focus our attention on the protective effect exerted by **Ru1** in neuroblastoma cells and, considering the ICP-AES results, cells were treated with 10 μM **Ru1** for 24 hours, followed by challenge with a pro-oxidant species for different time-periods depending on the experiment.

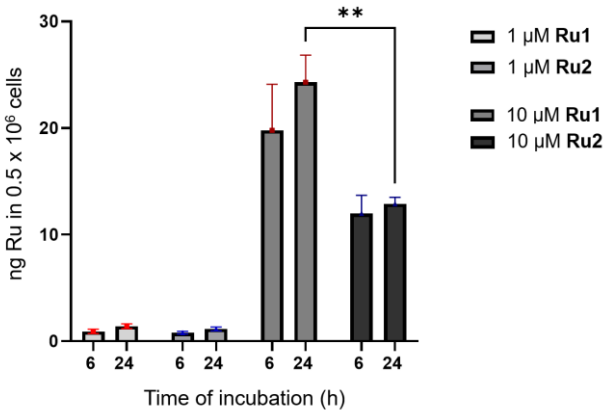

Figure 3. Ru1 and **Ru2** internalization in SH-SY5Y human neuroblasts. SH-SY5Y cells were treated with 1 or 10 μM **Ru1** and **Ru2** for 6 and 24 hours and analysed by ICP-AES to evaluate the concentration of Ru(II) internalised by cells. Data are reported as the mean ± SEM of three samples for each condition. Statistical analysis was by two-way ANOVA followed by Bonferroni post hoc test [** $p < 0.01$]

To set the pro-oxidant conditions, SH-SY5H cell viability was analysed by MTT assay upon H_2O_2 or CDDP or LPS treatment for 24 hours. As shown in Figure S19 (SI), while hydrogen peroxide challenge reduced cell viability at high concentrations (100-250 μM), CDDP showed a dose-dependent cytotoxic effect, which was lethal at high doses, whereas LPS didn't significantly show cytotoxic effects. Therefore, the following experiments were performed by employing 100-250 μM H_2O_2, and lower concentrations of CDDP (5-10 μM).

Once verified the internalization of **Ru1** into SH-SY5Y cells, we confirmed its negligible cytotoxicity by MTT assay as shown in Figure 4 (a-b), and we further tested its efficiency in preventing H_2O_2 and CDDP-induced cell death. Results indicated that incubation with 10 μM **Ru1** for 24 h significantly reverted H_2O_2 negative effect on cell viability, while it didn't show any effect on CDDP-induced cell death. CDDP was therefore excluded in the following experiments. On this basis, we tested the **Ru1** neuroprotective effect on H_2O_2 cytotoxicity in differentiated and undifferentiated SH-SY5Y cells and results were compared with the corresponding ones obtained for **Ru2** (Figure 4c-d).

Cells were differentiated for 7 days in 10 μM RA before being pre-treated with ruthenium compounds for 24 hours and challenged with H_2O_2 for other 24 hours. As shown in Figure 4c-d, both differentiated and undifferentiated cells show a reduction in cell viability with increasing concentrations of H_2O_2, with the differentiated cells being the most sensible to the pro-oxidant hydrogen peroxide since they showed an enhanced cell death even at lower concentrations. The negative effect on cell viability induced by H_2O_2 is then strongly reverted in the presence of **Ru1**, as witnessed, for example, by the recovering of c.ca 200% cell viability if compared to control for undifferentiated cells dosed with 100 μM H_2O_2 (Figure 4c). On contrary, **Ru2** could not prevent the hydrogen peroxide cytotoxicity.

The substantial differences found in the protective behaviour displayed by **Ru1** and **Ru2** can be reasonably explained by considering a combination of the different *cell-free* antioxidant and cellular internalization capabilities possessed by the two compounds. In particular, the higher protective effectiveness displayed by the former compound prompted us to focus our attention on the molecular mechanism responsible for **Ru1**-induced cell survival effect.

To this aim, we first inspected the hydrogen peroxide-induced pro-apoptotic effect and the eventual influence that **Ru1** has on this pathway. It's worthy to note that concentrations of H_2O_2 lower than 500 μM induce an apoptotic response, while higher concentrations lead to a necrosis cell death.[48] This can be also appreciated in Figure S20 (SI), where is reported a caspase 3

10.1002/chem.202400834

RESEARCH ARTICLE

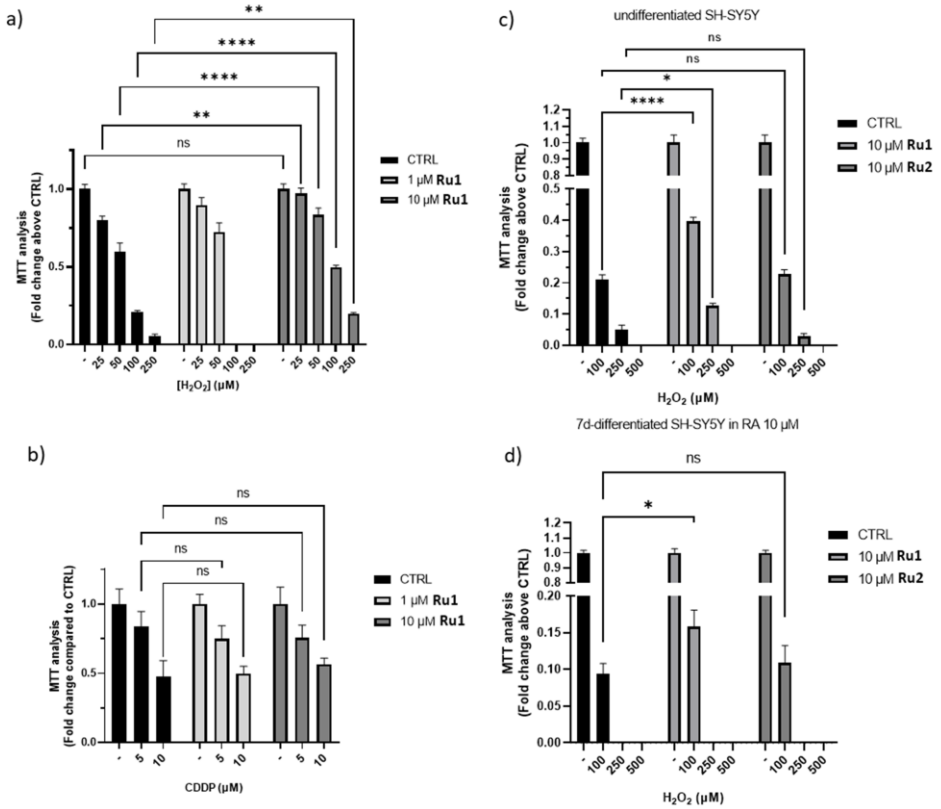

Figure 4. a-b) **Ru1** effect on cell viability. SH-SY5Y were seeded into 96-well plate and pre-treated with 1 μM or 10 μM **Ru1** for 24h, before adding H_2O_2 (25-50-100-250 μM, in a) or (CDDP 5-10 μM, in b) for 24 h. Experiments were performed in octuplicate, and data represent the mean ± SEM of at least three independent experiments. Statistical analysis was performed by two-way ANOVA followed by Bonferroni post hoc test [* $p < 0.05$, ** $p < 0.01$, *** $p < 0.001$, **** $p < 0.0001$]. c-d) **Ru1** and **Ru2** effect on cell viability in SH-SY5Y under different differentiation conditions. SH-SY5Y were seeded into 96-well plates and pre-treated with 1 μM or 10 μM of ruthenium complexes for 24 h, before adding H_2O_2 (100-250-500 μM) for 24 h. MTT assay was performed in undifferentiated cells (c) and in differentiated cells (d) cells. SH-SY5Y cells were differentiated by administration of 10 μM RA dissolved in 1% FBS media for 7 days. Data represent the mean ± SEM of at least three independent experiments. Statistical analysis was performed by two-way ANOVA followed by Bonferroni post hoc test [* $p < 0.05$, ** $p < 0.01$, not significant (ns)].

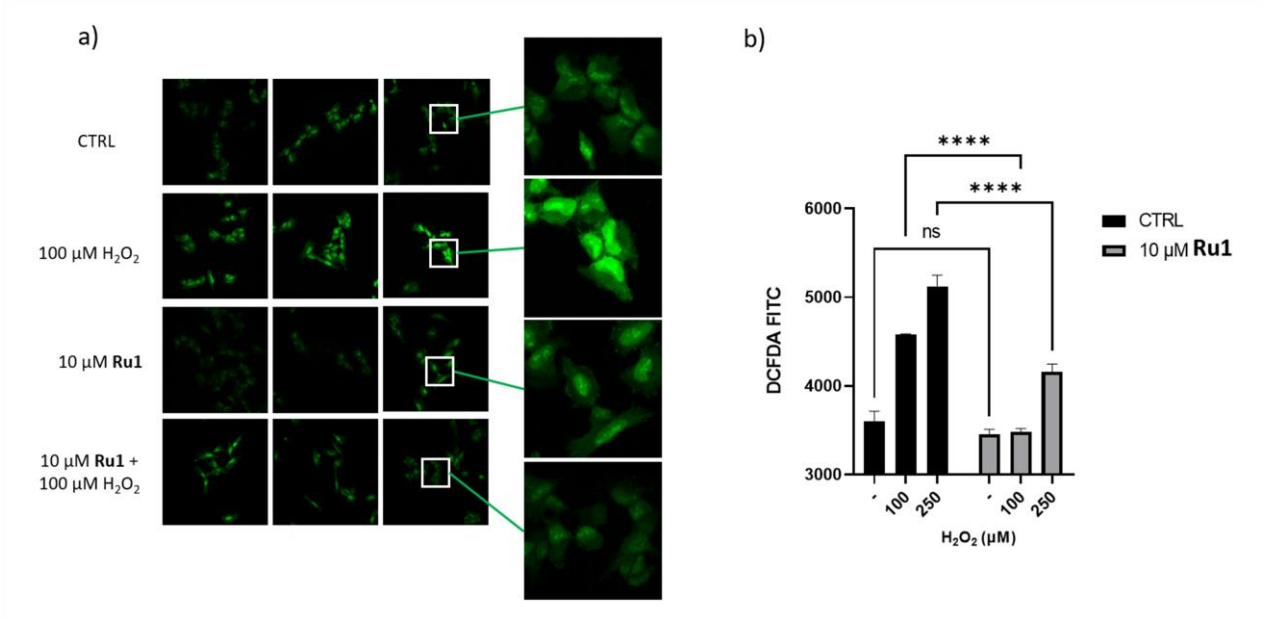

Figure 5. a) **Ru1** antioxidant activity on H_2O_2-mediated ROS production. SH-SY5Y were seeded on microscope slides and pre-treated with 10 μM **Ru1** for 18 h, before being challenged with 100 μM H_2O_2 for 6 h. Then slides were labelled with CM-H_2DCFDA (DCF) and fixed in paraformaldehyde, as described in the Materials and Methods section. Confocal analysis was performed using 63X oil immersion objective. b) **Ru1** antioxidant activity evaluated through flow cytometry. SH-SY5Y were pre-treated with 10 μM **Ru1** for 24 h, before being challenged with 100 or 250 μM H_2O_2 for 2 h. Cells were incubated with 1 μM CM-H_2DCFDA (DCF) for 15 minutes in dark. Data represent the mean ± SEM of at least two independent experiments. Statistical analysis was performed by two-way ANOVA followed by Bonferroni post hoc test [**** $p < 0.0001$, not significant (ns)].

10.1002/chem.202400834

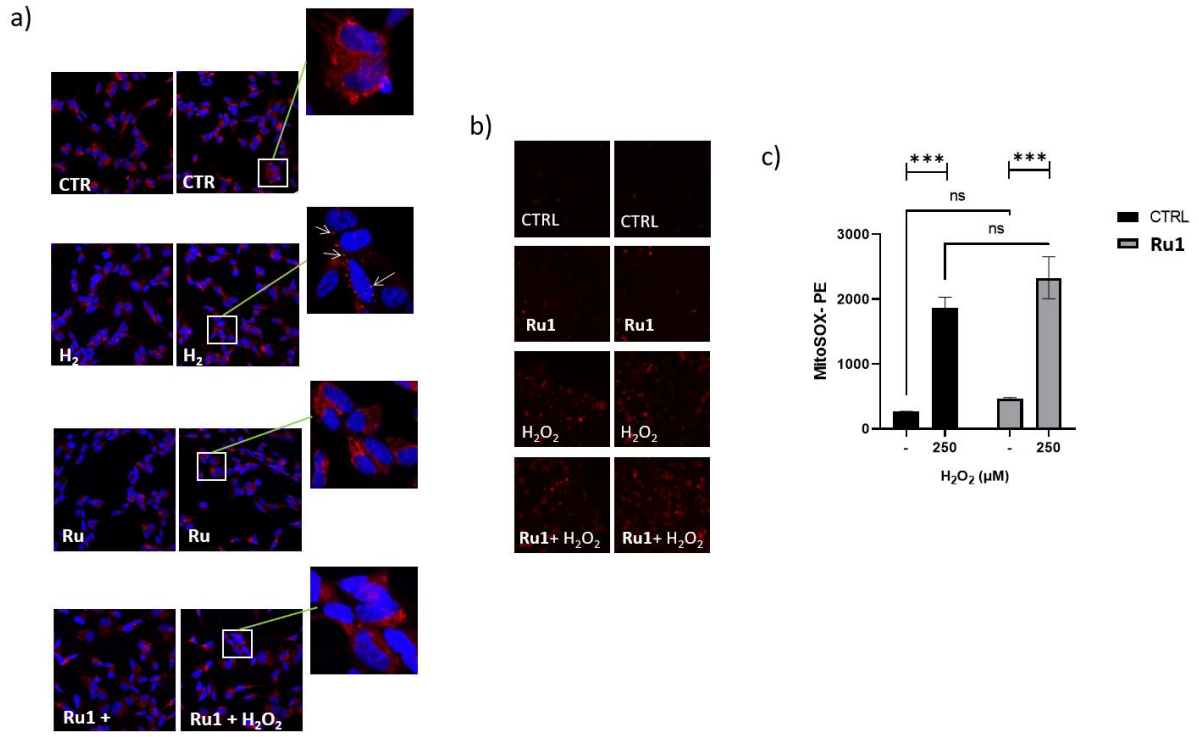

Figure 6. a) **Ru1** effect on mitochondrial function and superoxide content. SH-SY5Y cells were pre-treated with 10 μM **Ru1** for 18 h before being challenged with 250 μM H_2O_2 for 24h. Cells were labelled with MitoTracker Red CMXRos (a) or MitoSOX-PE (b) and fixed in paraformaldehyde, as described in the Materials and Methods section. Confocal analysis was performed using 63X oil immersion objective. Superoxide content was also evaluated by flow cytometry (c). SH-SY5Y were pre-treated with 10 μM **Ru1** for 24 h, before being challenged with 250 μM H_2O_2 for 2h. Cells were incubated with MitoSOX-PE. Data represent the mean ± SEM of at least two independent experiments. Statistical analysis was performed by two-way ANOVA followed by Bonferroni post hoc test [**** $p < 0.0001$, not significant (ns)].

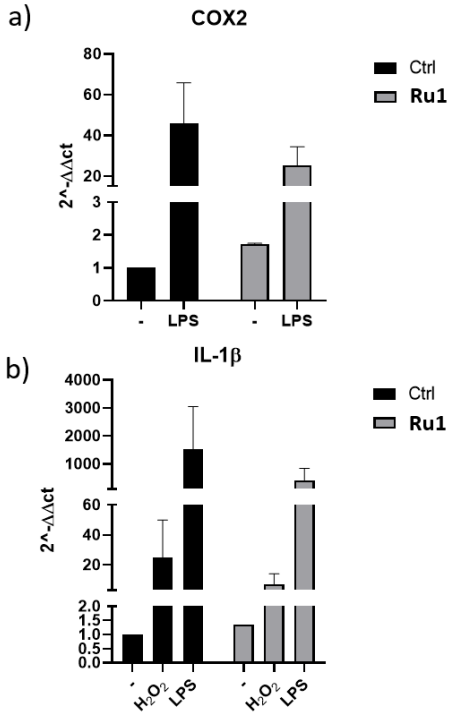

Figure 7. Anti-inflammatory activity of **Ru1** in undifferentiated SH-SY5Y. Cells were pre-treated with 10 μM **Ru1** for 18 h, before being challenged with 100 μM H_2O_2 or 3 μg/ml LPS for 3 and 24 h. The RNA expression levels of COX2 at 3 h treatments and IL-1β at 24 h treatments were assessed with real time PCR technique. The values are expressed as 2(-ΔΔCt) and normalized to β-Actin. Data are reported as mean ± SEM of at least two independent experiments.

activity assay performed on SH-SY5Y cells challenged with 100 μM H_2O_2, following pretreatment or not with the ruthenium compound. As shown in S20b (SI), in the absence of **Ru1**, hydrogen peroxide resulted in the cleavage of caspase 3 and PARP and therefore in the activation of the apoptotic response, while **Ru1** pre-treatment wasn't able to prevent H_2O_2 apoptotic-induction. These findings were further confirmed by fluorometric assay, performed to detect the activity of caspase 3. Samples were incubated with a specific caspase 3 substrate, which emits fluorescence once it is cleaved by the enzyme, thus making the fluorescence intensity an indirect measure of the enzyme activity (Fig. S20a). These data indicated that 100 μM H_2O_2 lead to the activation of caspase 3-mediated apoptotic cell death, which is not significantly reverted by 18 h **Ru1** pre-treatment. The antioxidant activity of **Ru1** has been then tested upon H_2O_2-mediated ROS generation by using the probe DCFH-DA in confocal microscope imaging to reveal the cytosolic ROS production. As shown in Figure 5a, SH-SY5Y challenged with 100 μM H_2O_2 for 6 h showed an enhancement in ROS levels, while **Ru1** pre-treatment for 18 h was efficient in preventing the H_2O_2-induced ROS increase. We further quantified ROS production induced by H_2O_2 by Fluorescence Activated Cell Sorting (FACS) using DCFH-DA to detect cytosolic ROS; the obtained results are reported in Figure S21 (SI) and Figure 5b. As shown, flow cytometry data confirmed the confocal images, indicating that **Ru1** pre-treatment was able to attenuate the production of ROS mediated by H_2O_2 at both concentrations of the pro-oxidant stimulus (100 and 250 μM).

Altogether these results indicate the capability of **Ru1** to prevent the formation of ROS induced by H_2O_2, confirming the antioxidant activity of this ruthenium complex in a biological model of neuroblasts cell line.

Mitochondrial dysfunction has been associated with several neurological diseases. Compounds that may be used to prevent or cure these disorders are gaining interest among the scientific

10.1002/chem.202400834

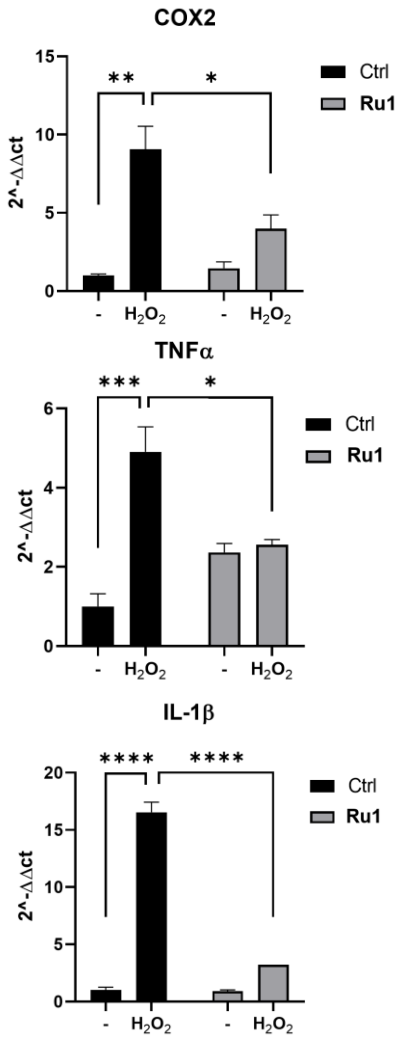

Figure 8. Anti-inflammatory activity of **Ru1** in differentiated SH-SY5Y. SH-SY5Y cells were differentiated using 10 µM RA dissolved in 1% FBS media for 7 days. Differentiated cells were pre-treated with 10 µM **Ru1** for 18 h, before being challenged with 100 µM H_2O_2 for 3 or 24 h. The RNA expression levels of COX2 at 3 h treatments, TNFα at 3 h treatments and IL-1β at 24 h treatments were assessed with Real-Time PCR technique. The values are expressed as 2(-ΔΔCt) and normalized to β-Actin. Data are reported as mean ± SEM of at least one experiment. Statistical analysis was performed by two-way ANOVA followed by Bonferroni post hoc test [* $p < 0.05$, ** $p < 0.01$, *** $p < 0.001$ **** $p < 0.0001$].

community.[49] Therefore, we determined the ROS-induced mitochondrial damage using the MitoTracker Red CMXRos probe. As we can see in Figure 6, H_2O_2 challenge for 24 h induced a fragmentation of cells mitochondria, while **Ru1** pre-treatment had a protective effect, preventing the mitochondrial fission. These results, which are quantified in Figure 6c, indicate that **Ru1** attenuates H_2O_2-induced mitochondrial damage, which can play an important role in the protection of SH-SY5Y from the cytotoxic effect of hydrogen peroxide.

Mitochondrial superoxide anion production was quantified both by confocal microscopy and FACS analysis upon H_2O_2 exposure using a mitochondrial superoxide indicator. H_2O_2 treatment induced mitochondrial superoxide production, which was not attenuated in the presence of **Ru1** (Figures 6b and 6c). **Ru1** antioxidant activity is therefore efficient in reducing cytosolic ROS but not mitochondrial superoxide anion production.

Recent studies suggest inflammation as a crucial role in the progression of neurodegeneration.[50,51] Activated microglia as well as other cells residing in the tissue can express pro-inflammatory cytokines, which have negative effects during neurodegenerative diseases. Therefore, the expression of inflammatory markers upon H_2O_2 or LPS challenge at RNA levels was also evaluated to reveal a possible anti-inflammatory effect of **Ru1**. Specifically, the gene expression of COX2, IL-1β upon H_2O_2 or LPS challenge for 3 or 24 h, was analysed in the presence or absence of **Ru1**. As reported in Figure 7, our data showed that enhanced expression of COX2 upon LPS treatment for 3 h, and IL-1 β expression after H_2O_2 and LPS challenge for 24 h was decreased by the pre-treatment with **Ru1**, even if the reduction was not statistically significant.

Lastly, the gene expression of the inflammatory markers was also analysed in differentiated SH-SY5Y cells upon H_2O_2 for 3 or 24 h in the presence or absence of **Ru1**. Data reported in Figure 8 showed an enhanced expression of COX2 and TNFα upon H_2O_2 treatment for 3 h, which was significantly reduced by the 18 h pre-treatment with **Ru1**. IL-1 β expression was enhanced as well by H_2O_2 challenge at 24 h and significantly reduced by **Ru1** pre-treatment, therefore highlighting the anti-inflammatory activity of **Ru1** in human differentiated neuroblasts.

Conclusion

Herein, we report on the synthesis, the chemical-physical characterization and the study of the antioxidant potential, of the novel ruthenium complex **Ru1**, featuring a tridentate dpby ligand and a non-innocent 2,3-DAN chelate in its chemical architecture. The ruthenium complex **Ru2**, with a tpy unit replacing dpby was also considered to evaluate the possible influence of the novel tridentate dpby ligand on the overall features of **Ru1**.

The insertion of dpby resulted in significant differences relative to the tpy-containing analogue, already in the synthetic routes for the preparation of ruthenium complexes, which were obtained by reaction of 2,3-DAN with the corresponding Ru(III) precursors $Ru(L)Cl_3$, (L = dpby (**Ru1**), tpy (**Ru2**). Indeed, contrary to $Ru(tpy)Cl_3$, obtained in ethanol according to procedures reported for the chelation of other nitrogen-containing ligands, the preparation of $Ru(dpby)Cl_3$ required to use 1,4-dioxane as solvent of reaction, unveiling a different reactivity of this ligand.

Given the presence of electroactive ligands into ruthenium complexes, their redox behaviour and antioxidant activity were inspected, prior to test their biological potential on neuroblastoma cells.

Oxidation-reduction potential (ORP) and cyclic voltammetry (CV) analysis indicated the redox activity of both ruthenium complexes, in which the contribution of 2,3-DAN appears to be preserved. On the other side, their capacity to act as ROS-scavenger was investigated by using the DPPH· scavenger activity assay, which highlighted significant differences among the two complexes. In particular, **Ru1** emerged to be the most efficient towards the neutralization of DPPH radical, with an effectiveness comparable to that of 2,3-DAN, whereas a *c.ca* 2-fold lower activity was displayed by **Ru2**, comparable to that induced by the reference compound Trolox.

Taken together these results proved that the electroactivity of the non-innocent 2,3-DAN ligand is maintained upon its inclusion into ruthenium scaffolds, and that the presence of different tridentate ligands in their structures may influence their relative antioxidant properties. In this respect, further Natural Bond Orbital (NBO) analysis led us to speculate a possible role played by the different electronic nature of tridentate ligands in modulating the activity imparted by the Ru(II)-coordinated 2,3-DAN.

Following the characterization of the antioxidant activities of the two ruthenium compounds by chemical assay we then inspected their possible use as antioxidant agents in the treatment of neurodegenerative diseases.

Their neuroprotective effect was evaluated in the neuroblastoma cell line SH-SY5Y upon pro-apoptotic/pro-oxidant molecules challenge. H_2O_2 challenge caused a reduction in cell viability, the activation of the apoptotic cell death, mitochondrial disfunctions, enhanced cytosolic and mitochondrial ROS production and increased expression of inflammatory markers. ICP-AES

10.1002/chem.202400834

experiments evidenced a superior capacity of **Ru1** to be internalized by SH-SY5Y cells if compared to the tpy-containing analogue **Ru2**, thus highlighting the beneficial role played by the novel dpby chelate. Among the two ruthenium complexes, and in good agreement with the different DPPH• radical scavenging abilities and cellular internalization exhibited by the two compounds, only **Ru1** 18 h pre-treatment (time for pre-treatment was chosen on the basis of ICP internalization analysis) reduced the H_2O_2-induced cytotoxicity, along with cytosolic ROS production and mitochondrial fission. This confirmed the key role played by the tridentate dpby ligand in affecting the biological behaviour of the resulting ruthenium complex, and also focused our attention on further investigating the molecular mechanism responsible for **Ru1**-induced cell survival effect.

The cytosolic antioxidant activity of **Ru1** wasn't found efficient to reduce mitochondrial ROS nor the apoptotic response induced by H_2O_2. Moreover, **Ru1** wasn't able to revert the CDDP cytotoxicity. This latter result could be explained by the fact that CDDP can bind directly to DNA leading to a ROS-independent damage, and therefore making the antioxidant activity of the ruthenium complex ineffective. Lastly, the anti-inflammatory activity of **Ru1** was also explored; results showed that 18 h **Ru1** pre-treatment was able to reduce some of the investigated inflammatory markers upon LPS or H_2O_2 challenge in differentiated neuroblasts.

In conclusion, these original results show that antioxidant ruthenium(II) complex, **Ru1**, or parent ruthenium complexes, could be potentially useful as new pharmacological tools in neurodegenerative diseases associated with a high oxidative stress. Moreover, they specially prove that the electroactivity of otherwise unusable ligands, such as 2,3-DAN, can be preserved upon its insertion into ruthenium complexes, whose overall antioxidant properties are likely the result of a non-trivial modulation of bioactivities of ligands combined in their chemical architectures.

Experimental section

Materials. All chemicals were purchased from Aldrich, in the highest quality commercially available. The solvents were RP grade, unless otherwise indicated.

Synthesis of the precursor Ia. To a warmed solution (40°C) of dpby (100 mg, 0.29 mmol) in 15 mL of deaerated 1,4-dioxane was added a solution of ruthenium chloride trihydrate (60 mg, 0.29 mmol) dissolved in 15 mL of deaerated 1,4-dioxane. The reaction mixture was stirred at reflux overnight and after cooling at *r.t.* the brown precipitate was collected by filtration washing with ethanol and diethyl ether and then dried in vacuum to obtain complex Ia as a brown solid. The product was utilized in the following synthetic step without further purification.Yield of 87%. IR ν 3070, 3037 cm^{-1} (C-H stretching modes), 1662 cm^{-1} (C=N stretch.), 1440-1365 cm^{-1} (stretch. vibrations of pyridine/benzene ring), 1147 cm^{-1} (C-O-C asym. stretch.), 1076 (C-O-C symm. stretch.). IR band assignemt performed according to literature.[52]

Synthesis of 2,6-bis(4-methyl-2-benzossazolyl)pyridine (dpby). 2-amino-3-methylphenol (**1**) (6.16 g, 50.0 mmol) and pyridine-2,6-dicarboxylic acid (**2**) (4.18 g, 25.0 mmol) were suspended in polyphosphoric acid (40 g) and heated overnight at 160°C. The reaction mixture was cooled to room temperature and then poured into 1.00 dm^3 of water at 0°C. After neutralization with Na_2CO_3, the mixture was filtered, and the solid residue was washed with methanol and dried under reduced pressure obtaining the pure product as white crystalline solid (6.48 g, 76%). ^{1}H-NMR ($CDCl_3$, 25°C) δ 8.55 (2H, d, *J* = 7.8 Hz), 8.10 (1H, t, *J* = 7.8 Hz), 7.55 (2H, d, *J* = 8.1 Hz), 7.34 (2H, t, *J* = 7.6 Hz), 7.22 (2H, d, *J* = 7.4 Hz, 2.74 (6H, s) ppm.^{13}C-NMR: ($CDCl_3$, 25 °C) δ 160.0, 151.0, 146.8, 141.1, 138.1, 131.4, 126.0, 125.4, 124.9, 108.8, 16.5 ppm.

Synthesis of the ruthenium complex [(dbpy)Ru(nqdi)Cl]PF_6 (Ru1). Complex **Ru1** was synthetized by dropping a solution of 2,3-DAN (39.5 mg, 0.25 mmol) in 15 mL of deaerated ethanol into a suspension of compound **Ia** (80 mg, 0.15 mmol) in 10 mL of the same solvent. TEA (triethylamine, 253 mg, 2.5 mmol) was then added, and the reaction mixture was stirred at *r.t.* for 30 min. The subsequent addition of a solution of KPF_6 0.1M (8 mL) allowed the precipitation of complex **Ru1** as hexafluorophosphate salt, which was collected by filtration and washed with water and diethyl ether affording the final complex as a purple solid. Yield 84%. ^{1}H-NMR (400 MHz, $(CD_3)_2CO$): δ 13.78 (bs, **-NH**), 12.2 (bs, **-NH**), 8.95 (d, J = 8.0 Hz, 2H, **H3'**), 8.75 (t, J = 8.4 Hz, 1H, **H4'**), 8.58 (s, 1H, $\mathbf{H_g}$), 7.74 - 7.67 (m, 3H, **H7** and $\mathbf{H_c}$ or $\mathbf{H_f}$), 7.48 (t, J=8.4 Hz, 2H, **H6**), 7.31-7.20 (m, 4H, **H5**, $\mathbf{H_b}$ and $\mathbf{H_c}$ or $\mathbf{H_f}$), 6.97 (m, 2H, $\mathbf{H_d}$ and $\mathbf{H_e}$), 2.57 (s, 6H, $-CH_3$) ppm. ^{13}C-NMR (100 MHz, $(CD_3)_2CO$): δ 171.2, 171.1, 165.0, 163.1, 150.9, 145.4, 137.4, 130.4, 129.7, 129.3, 129.1, 128.6, 128.0, 127.1, 116.0, 115.2, 110.4, 18.7 ppm. ESI-MS: calcd for $C_{31}H_{23}ClN_5O_2Ru$ $[M]^+$ 634.06, found 634.5 (m/z = 1).

Synthesis of the ruthenium complex [(tpy)Ru(nqdi)Cl]PF_6 (Ru2). This complex was obtained by adopting a similar procedure to a synthetic route recently reported,[26] following the preparation of the intermediate **IIa**, obtained according to literature.[31,53] Briefly, a solution of 2,3-DAN (23 mg, 0.15 mmol) in 10 mL of deaerated ethanol was dropped into a suspension of compound **IIa** (80 mg, 0.15 mmol) in 10 mL of the same solvent. TEA (178 mg, 1.75 mmol) was then added, and the reaction mixture was heated to 70°C and stirred vigorously for 10 min. After cooling to *r.t.*, a solution of KPF_6 0.1M (5 mL) was added while stirring. The mixture was then concentrated under reduced pressure until the ruthenium complex completely precipitated, as the hexafluorophosphate salt **Ru2**. The purple solid was collected by filtration, washed with water and diethyl ether and purified by flash chromatography on silica gel (eluent: dichloromethane:methanol 20:1). Yield 32%. ^{1}H-NMR (400 MHz, $(CD_3)_2CO$): δ 13.68 (bs, **-NH**), 11.61 (bs, **-NH**), 8.92 (d, J = 8.4 Hz, 2H, **H3'**), 8.68 (d, J = 8.0 Hz, 2H, **H3**), 8.51 (t, J = 8.0 Hz, 1H, **H4'**), 8.23 (s, 1H, $\mathbf{H_g}$), 8.08 (t, J = 8.0 Hz, 2H, **H4**), 7.73 - 7.67 (m, 1H, $\mathbf{H_c}$ or $\mathbf{H_f}$), 7.48 - 7.39 (m, 6H, $\mathbf{H_5}$, $\mathbf{H_6}$, $\mathbf{H_b}$ and $\mathbf{H_c}$ or $\mathbf{H_f}$), 7.05 (m, 2H, $\mathbf{H_d}$ and $\mathbf{H_e}$) ppm. ^{13}C-NMR (100 MHz, $(CD_3)_2CO$): δ 169.6, 164.8, 158.6, 156.9, 154.5, 139.4, 138.5, 132.9, 132.8, 129.6, 129.2, 128.0, 127.5, 124.2, 123.8, 117.2, 117.1, 114.4, 114.3 ppm.

UV-vis absorption and fluorescence analysis. Absorption spectra were registered on a Perkin-Elmer Lambda 6 spectrophotometer. Fluorescence spectra were recorded on a Perkin-Elmer LS55 spectrofluorimeter, by using an excitation wavelength of 411 nm.

NMR and FTIR analysis. NMR spectra were collected with a Bruker 400 MHz spectrometer. FTIR analysis was performed in attenuated total reflectance (ATR) mode with a IRAffinity-1S (SHIMADZU) equipped with the ATR sampling accessory (MIRacleTM PIKE Technologies).

Voltammetry analysis (CV). Cyclic voltammetry (CV) at a Glassy Carbon Electrode (GCE) surface, from -0.5 to +2.5 V, using a scan rate 25 mV/s. The electrochemical set-up comprised a three-electrode system: MeCN(Ag/$AgNO_3$) as Reference Electrode (RE), a Pt wire as Counter Electrode (CE), and a Glassy Carbon Working Electrode (WE). Samples were prepared at a concentration of 1 mM in acetonitrile, using 0.1 M Bu_4NClO_4 as supporting electrolyte. AUTOLAB-PGSTAT10 potentiostat/galvanostat was used to perform the measurements.

ORP analysis. Measurements of the Oxidation-reduction potential (ORP), of ruthenium compounds, 2,3-DAN and Trolox solutions were performed as previously described,[54] by using an ORP electrode (*HI3148B ORP, Hanna® Instruments, Padova, Italy*) combined with a pH/ORP meter (*HI5222 bench meter Hanna® Instruments, Padova, Italy*). Before measurements, the electrode was calibrated with two redox standard solutions (*HI7021 and HI7022, Hanna® Instruments, Padova, Italy*). Acetonitrile (*Supelco*) was obtained from Sigma-Aldrich.

DPPH• free radical scavenging activity assay. The free radical scavenging activities of ruthenium complexes as well as of free ligands (2,3-DAN, tpy and dbpy), were evaluated using the bleaching of purple-coloured methanolic solutions of α,α-diphenyl-β-picrylhydrazyl (DPPH•), according to previously reported procedures[55,56] and by using Trolox as a positive control. Each compound tested was progressively added to freshly prepared methanolic solutions of DPPH• (75 μM, 2 mL) to result in final concentrations of tested compounds between 0-14 μM, and the resulting solutions were stirred at room temperature while kept under dark conditions. After 30 min of incubation in the dark, spectra were collected by using a methanolic solution containing the tested compound at the same concentration as that in the measurement cuvette as a blank reference. The DPPH scavenging activity (%DPPH•) was calculated using the following formula:

$$\%DPPH\cdot = \frac{A_0 - A}{A_0} 100$$

where A_0 and A are respectively the absorbance values at 516 nm of DPPH in the absence and in the presence of the increasing concentrations of the tested compound. EC_{50} values refer to the substrate concentration that reduces by half the concentration (colour) of DPPH• and were extrapolated from the linear regression analysis of the %DPPH• values reported as a function of the substrate concentrations (Figure S17, SI).

Singlet oxygen sensitization by DHN probe. The singlet oxygen sensitization by ruthenium complexes was evaluated by employing 1,5-dihydroxynaphthalene (DHN) as an indirect singlet oxygen reporter, according to already reported procedures.[57-59] In presence of $^1O_2$, DHN is promptly and quantitatively oxidized to its photoproduct 5-hydroxy-1,4-naphthalenedione (Juglone), a process that can be easily followed by UV-vis spectroscopy by monitoring the decrease of the DHN absorption band at λ_{max} 297 nm and the simultaneous increase of the broad Juglone band centered at *ca*. 427 nm. Therefore, acetonitrile solutions of the tested compounds (10 μM) and DHN (3.3 x 10^{-4} M) were subjected to increasing irradiation times (LED light, λ > 430 nm, 30 W) and UV-Vis spectra were collected by using as a blank reference a solution containing the tested ruthenium complex at the same concentration of the measuring cuvette.

SH-SY5Y cell culture. Human SH-SY5Y neuroblastoma cell line (ATCC, CRL-2266) was purchased from LGC (LGC Standards, LGC Group) European partner of ATCC. Cells were maintained in 1:1 DMEM:F12 HAM nutrient mixture medium (Sigma-Aldrich, St. Louis, MO, USA), supplemented with 10% FBS, 100 U/mL penicillin/streptomycin, and 2 mM L-glutamine, at 37°C in 5% CO2 atmosphere. SH-SY5Y cells are commonly used in neurosciences as an in vitro model to study molecular mechanisms of neurodegenerative diseases such as Alzheimer e Parkinson. They can be used as undifferentiated cells, or they can be easily induced to express a neuron like phenotype. The differentiation process was induced at 70% of confluency, shifting the cells to 1% FBS media and adding 10 μM retinoic acid (RA). Cells were maintained in the differentiation media for 7 days, which was changed every two days.

MTT reduction assay. The MTT (3-(4,5-dimethylthiazol-2-yl)-2,5-diphenyltetrazolium bromide) assay is a standard colorimetric test for assessing cell viability. Cells were plated in 96-multiwell at least 5 wells per condition. After the treatment cells were washed twice with PBS, 200 μL MTT 1X solution was added to each well and cells were then incubated at 37°C in the dark. Depending on the cell line, the MTT 1X solution was prepared by diluting 1:10 the stock solution in RPMI DMEM or DMEM/F12 without phenol red, which can interfere with the incorporation of the dye. Living cells can uptake the yellow dye, by endocytosis, and the NAD(P)H-dependent cellular oxidoreductase enzyme reduces the tetrazolium dye MTT to its insoluble formazan, which has a purple colour. After the incubation time, MTT was removed, and cells were lysate with DMSO 100% (150 μL /well). This leads to the solubilisation of the formazan crystals and the colour intensity of each well was quantified by a spectrophotometer at 595 nm. The degree of cell viability is dependent on the degree of the formazan production and directly proportional to the intensity of the purple colour.

Caspase-3 Activity Assay. SH-SY5Y cells were seeded in 6-well plates and after 24 h were subjected to different treatments depending on the experimental conditions. After the treatments, cells were washed twice with PBS and collected in a buffer containing Tris-HCl 20 mM pH 7.4, NaCl 250 mM, EDTA 2 mM, Triton X-100 0.1%, DTT 1 mM, Na3VO4, PMSF 0.5 mM and protease inhibitor cocktail (Sigma-Aldrich, USA). Samples were left in ice for 30 minutes before being lysed by two sonication cycles of 20 seconds and centrifugated at 16.000xg, 5 minutes 4°C. Protein lysates (30 μg) were resuspended in a buffer containing Hepes-KOH 50 mM pH 7, glycerol 10%, EDTA 2 mM, 3-[(3-cholomidopropyl)-dimethylammonio]-1-propanesulfunate 0.1% plus DDT 10 μM and Ac-DEVD-AFC 50 μM substrate (Cayman Chemical Company, MI, USA). Caspase-3 activity depends on Asp216 cleavage and the tetrapeptide was used to quantify it. The reaction was monitored quantitatively by measuring shift in fluorescence upon cleavage. Ac-DEVD-CHO (200 nM) specific inhibitor of caspase-3 (Cayman Chemical Company, MI, USA) was used as a negative control, incubated with all cell lysates 15 minutes before adding the substrate. After 2 hours incubation at 37°C in the dark, samples were measured at 505 nm wavelength with 400 nm excited wavelength by fluorescence spectrometer (Cary Eclipse Fluorescence Spectrometer, Bio-Rad, CA, USA).

Laser-Scanning Confocal Microscopy. SH-SY5Y cells were seeded into microscope slides and after 24 h were subjected to different treatments depending on the experimental conditions. MitoTracker Red CMXRos (#M7512; Ex/Em: 579/599 nm) and CM-H2DCFDA (#C6827; Ex/Em:492–495/517–527 nm) probes (Invitrogen, Thermo Fisher Scientific INC,Waltham, MA, USA) were used to detect the mitochondrial membrane potential and ROS production, respectively. After diffusing through the cell membrane, DCFH-DA probe is hydrolysed by esterase in DCFH and oxidised by radical species forming DCF, a fluorescent compound which indicates the presence of cytosolic ROS. MitoSOX Red mitochondrial superoxide indicator (#M36008; Ex/Em: ~396/610 nm; Invitrogen, Thermo Fisher Scientific INC,Waltham, MA, USA) was employed to detect mitochondrial superoxide production. The probes were diluted in RPMI or DMEM medium without phenol red or PBS, incubated for 30 min at 37°C in dark and then fixed in 2% paraformaldehyde, as suggested by the manufacturer's instruction. Ru(II) complexes excitation was performed using a 405 nm laser diode, acquiring emission in the range of 600/620 nm.

Western blot analysis. SH-SY5Y lysates were quantified for total protein content by the Bradford Protein assay, resuspended in Leammli's sodium dodecyl sulphate (SDS) sample buffer, and subjected to SDS-PAGE and transferred to PVDF membranes. Anti-caspase 3 and anti-PARP antibodies were purchased from Cell Signaling Technology (Danvers, MA, USA).

Real-Time PCR. SH-SY5Y cells were plated in 6-well plates (500.000 cells/well), the day after cells were shifted to 1% FBS media and treated with 10 μM of the antioxidant Ru1 for 18 h. Subsequently, 100 μM H_2O_2 or 3 ng/ml LPS were added for 3 and 24 h. TaqMan Gene expression assays specific for inflammatory cytokines (IL-1β, IL-6, TNFα and COX2) were purchased from Thermo Fisher Scientific INC (MA, USA).

ICP-AES Measurements. In order to study the internalization of Ru(II) complexes in A2780, A-431 or SH-SY5Y cells the ICP-AES technique was performed. It is an analytical technique used to determine the concentration of a variety of inorganic metallic and

non-metallic substances. Cells were seeded into p100 petri dishes and after reaching the desired confluence were treated with different Ru(II) complexes and incubated at 37°C in dark depending on the experimental conditions. Then, cells were washed twice in cold PBS, collected in ice by scraping the surface of the plate with 1 ml of PBS into 15 ml tubes, and centrifuged at 1000xg for 5 minutes. Pellets were maintained at -80°C until the ICP analysis was performed. Ru content in the samples was determined using an axial Varian 720-ES Inductively Coupled Plasma Atomic Emission Spectrometer (ICP-AES). Measurements were performed in triplicate.

Fluorescence-activated cell sorting (FACS). SH-SY5Y cells were labelled with the specific probes in order to quantify the cytosolic or mitochondrial ROS production upon H_2O_2 exposure in the presence/absence of Ru1. SH-SY5Y were pre-treated with Ru1 for 18 h before being exposed to 100-250 µM H_2O_2 for 2 h. Cells were detached with Trypsin–EDTA solution (Sigma- Aldrich) and incubated with 1 µM CM-H2DCFDA for 15 minutes in suspension in dark in order to identify cytosolic ROS or labelled in adhesion with 2.5 µM MitoSOX Red mitochondrial superoxide indicator for 10 minutes in order to quantify mitochondrial ROS production, then detached with Trypsin– EDTA solution (Sigma-Aldrich). Cell fluorescence intensity was measured with a FACSCanto flow- cytometer (Becton– Dickinson, Franklin Lakes, NJ, USA).

Statistical analysis. In order to obtain a statistical analysis of the experimental results, Student's t-test and one-way or two-way analysis of variance (ANOVA), followed by Bonferroni post-hoc analysis, were performed. A level of $p<0.05$ was considered statistically significant. Densitometry analysis of Western Blot images was carried out with ImageJ software and for all the graphical images, GraphPad Prism v8.4.3 (GraphPad Software, La Jolla, CA, USA) was used.

Acknowledgements

The publication was made with the contribution of the researcher L. C. with a research contract co-funded by the European Union - PON Research and Innovation 2014-2020 in accordance with Article 24, paragraph 3a), of Law No. 240 of December 30, 2010, as amended, and Ministerial Decree No. 1062 of August 10, 2021. The authors acknowledge MIUR for "*Progetto Dipartimenti di Eccellenza 2018–2022*" allocated to the Department of Chemistry "*Ugo Schiff*". The authors would like to thank Mirko Severi from the Department of Chemistry "*Ugo Schiff*" for the ICP-AES analysis.

Keywords: Ruthenium polypyridyl complexes • antioxidant • neuroblastoma cells • benzoxalzole derivatives • Anti-inflammatory

References:

[1] A.Singh, R. Kukreti, L. Saso, S. Kukreti, *Molecules* **2019**, *24* (8), 1583. https://doi.org/10.3390/molecules24081583.
[2] E. Niedzielska, I. Smaga, M. Gawlik, A. Moniczewski, P. Stankowicz, J. Pera, M. Filip, *Mol. Neurobiol.* **2016**, *53* (6), 4094-4125. https://doi.org/10.1007/s12035-015-9337-5.
[3] V. Raimondi, F. Ciccarese, V. Ciminale, *Br. J. Cancer* **2020**, *122* (2), 168-181. https://doi.org/10.1038/s41416-019-0651-y.
[4] P. R. Angelova, A. Y. Abramov, *FEBS Letters*. **2018**. https://doi.org/10.1002/1873-3468.12964.
[5] M. W. S. Campelo, R. B. Oriá, L. G. de França Lopes, G. A. de C. Brito, A. A. dos Santos, R. C. de Vasconcelos, F. O. N. da Silva, B. N. Nobrega, M. T. Bento-Silva, P. R. L. de Vasconcelos, *Neurochem. Res.* **2012**, *37* (4), 749-758. https://doi.org/10.1007/s11064-011-0669-x.
[6] F. V. Gama Justi, G. Araújo Matos, J. de Sá Roriz Caminha, C. Rodrigues Roque, E. Muniz Carvalho, M. W. Soares Campelo, L. Belayev, L. Gonzaga de França Lopes, R. Barreto Oriá, *J. Pharmacol. Exp. Ther.* **2022**, *380* (1), 47-53. https://doi.org/10.1124/jpet.121.000798.
[7] P. Singh, B. Sharma, *Curr. Neurovasc. Res.* **2016**, *13* (1), 10-21. https://doi.org/10.2174/1567202612666151026105610.
[8] J. Kwak, J. Woo, S. Park, M. H. Lim, *J. Inorg. Biochem.* **2023**, *238*, 112053. https://doi.org/10.1016/j.jinorgbio.2022.112053.
[9] A. Rilak Simović, R. Masnikosa, I. Bratsos, E. Alessio, *Coord. Chem. Rev.* **2019**, *398*, 113011. https://doi.org/10.1016/j.ccr.2019.07.008.
[10] R. Kanaoujiya, Meenakshi, S. Srivastava, R. Singh, G. Mustafa, *Mater. Today Proc.* **2023**, *72*, 2822-2827. https://doi.org/10.1016/j.matpr.2022.07.098.
[11] D. Sun, W. Zhang, M. Lv, E. Yang, Q. Zhao, W. Wang, *Bioorg. Med. Chem. Lett.* **2015**, *25* (10), 2068-2073. https://doi.org/10.1016/j.bmcl.2015.03.090.
[12] J. E. Waters, L. Stevens-Cullinane, L. Siebenmann, J. Hess, *Curr. Opin. Microbiol.* **2023**, *75*, 102347. https://doi.org/10.1016/j.mib.2023.102347.
[13] G. E. Giacomazzo, M. Schlich, L. Casula, L. Galantini, A. Del Giudice, G. Pietraperzia, C. Sinico, F. Cencetti, S. Pecchioli, B. Valtancoli, L. Conti, S.Murgia, C. Giorgi, *Inorg. Chem. Front.* **2023**, *10* (10), 3025-3036. https://doi.org/10.1039/D2QI02678C.
[14] L. Conti, G. E. Giacomazzo, B. Valtancoli, M. Perfetti, A. Privitera, C. Giorgi, P. S. Sfragano, I. Palchetti, S. Pecchioli, P. Bruni, F. Cencetti, *Int. J. Mol. Sci.* **2022**, *23* (21), 13302. https://doi.org/10.3390/ijms232113302.
[15] T. Le Gall, G. Lemercier, S. Chevreux, K.Tücking, J. Ravel, F. Thétiot, U. Jonas, H. Schönherr, T. Montier, *ChemMedChem* **2018**, *13* (20), 2229–2239. https://doi.org/10.1002/cmdc.201800392.
[16] S.-J.Tang, M.-F. Wang, R. Yang, M. Liu, Q.-F. Li, F. Gao, *Inorg. Chem.* **2023**, *62* (21), 8210-8218. https://doi.org/10.1021/acs.inorgchem.3c00585.
[17] S. A. McFarland, A. Mandel, R. Dumoulin-White, G. Gasser, *Curr. Opin. Chem. Biol.* **2020**, *56*, 23-27. https://doi.org/10.1016/j.cbpa.2019.10.004.
[18] Bonnet, S. Ruthenium-Based Photoactivated Chemotherapy. *J. Am. Chem. Soc.* **2023**, *145* (43), 23397–23415. https://doi.org/10.1021/jacs.3c01135.
[19] G. E. Giacomazzo, L. Conti, A. Guerri, M. Pagliai, C. Fagorzi, P. S. Sfragano, I. Palchetti, G. Pietraperzia, A. Mengoni, B. Valtancoli, C. Giorgi, *Inorg. Chem.* **2022**, *61* (18), 6689-6694. https://doi.org/10.1021/acs.inorgchem.1c03032.
[20] G. E. Giacomazzo, L. Conti, C. Fagorzi, M. Pagliai, C. Andreini, A. Guerri, B. Perito, A. Mengoni, B. Valtancoli, C. Giorgi, *Inorg. Chem.* **2023**, *62* (20), 7716-7727. https://doi.org/10.1021/acs.inorgchem.3c00214.
[21] H. D. Cole, J. A. Roque, G. Shi, L. M. Lifshits, E. Ramasamy, P. C. Barrett, R. O Hodges, C. G. Cameron, S. A. McFarland, *J. Am. Chem. Soc.* **2022**, *144* (22), 9543-9547. https://doi.org/10.1021/jacs.1c09010.
[22] G.-B. Jiang, Y.-Y. Xie, G.-J. Lin, H.-L. Huang, Z.-H. Liang, Y.-J. Liu, *J. Photochem. Photobiol. B Biol.* **2013**, *129*, 48-56. https://doi.org/10.1016/j.jphotobiol.2013.09.009.
[23] M. Małecka, A. Skoczyńska, D. M. Goodman, C. G. Hartinger, E. Budzisz, *Coord. Chem. Rev.* **2021**, *436*, 213849. https://doi.org/10.1016/j.ccr.2021.213849.
[24] P. Srivastava, R. Mishra, M. Verma, S. Sivakumar, A. K. Patra, *Polyhedron* **2019**, *172*, 132-140. https://doi.org/10.1016/j.poly.2019.04.009.
[25] P. Srivastava, P. N. Tripathi, P. Sharma, S. N. Rai, S. P. Singh, R. K. Srivastava, S. Shankar, S. K. Shrivastava, *Eur. J. Med. Chem.* **2019**, *163*, 116-135. https://doi.org/10.1016/j.ejmech.2018.11.049.
[26] M. Međedović, A. Rilak Simović, D. Ćoćić, L. Senft, S. Matić, D. Todorović, S. Popović, D. Baskić, B. Petrović, *Dalt. Trans.* **2023**, *52* (5), 1323-1344. https://doi.org/10.1039/D2DT02993F.
[27] Saba A. Gheni, Mudheher M. Ali, Goh C. Ta, Hannah J. Harbin, Saad A. Awad, *ACS Chem. Health Saf.* **2024**, 31(1), 8-21. https://doi.org/10.1021/acs.chas.3c00073
[28] G. Ambrosi, M. Fanelli, P. Paoli, M. Formica, D. Paderni, P. Rossi, M. Micheloni, L. Giorgi, V. Fusi, *Dalt. Trans.* **2020**, *49* (22), 7496-7506. https://doi.org/10.1039/C9DT03910D.
[29] D. Paderni, G. Barone, L. Giorgi, M. Formica, E. Macedi, V. Fusi, *Dalt. Trans.* **2023**, *52* (12), 3716-3724. https://doi.org/10.1039/D3DT00140G.
[30] D. Paderni, L. Giorgi, M. Voccia, M. Formica, L. Caporaso, E. Macedi, V. Fusi, *Chemosensors* **2022**, *10* (5), 188. https://doi.org/10.3390/chemosensors10050188.
[31] B. P. Sullivan, J. M. Calvert, T. J. Meyer, *Inorg. Chem.* **1980**, *19* (5), 1404-1407. https://doi.org/10.1021/ic50207a066.
[32] A. Singh, B. Mondal, *Inorganica Chim. Acta* **2010**, *363* (13), 3145-3150. https://doi.org/10.1016/j.ica.2010.05.042.
[33] S. C. Yu, S. Hou, W. K. Chan, *Macromolecules* **1999**, *32* (16), 5251-5256. https://doi.org/10.1021/ma990056h.
[34] T. Jüstel, J. Bendix, N. Metzler-Nolte, T. Weyhermüller, B. Nuber, K. Wieghardt, *Inorg. Chem.* **1998**, *37* (1), 35-43. https://doi.org/10.1021/ic970850o.
[35] S. Maji, S. Patra, S. Chakraborty, D. Janardanan, S. M. Mobin, R. B. Sunoj, G. K. Lahiri, *Eur. J. Inorg. Chem.* **2007**, *2007* (2), 314-323. https://doi.org/10.1002/ejic.200600830.

[36] P. Čanović, A. R. Simović, S. Radisavljević, I. Bratsos, N. Demitri, M. Mitrović, I. Zelen, Ž. D. Bugarčić, *J. Biol. Inorg. Chem.* **2017**. https://doi.org/10.1007/s00775-017-1479-7.
[37] G. A. Parada, L. A. Fredin, M.-P. Santoni, M. Jäger, R. Lomoth, L. Hammarström, O. Johansson, P. Persson, S. Ott, *Inorg. Chem.* **2013**, *52* (9), 5128-5137. https://doi.org/10.1021/ic400009m.
[38] M. T. Rupp, N. Shevchenko, G. S. Hanan, D. G. Kurth, *Coord. Chem. Rev.* **2021**, *446*, 214127. https://doi.org/10.1016/j.ccr.2021.214127.
[39] A. Rilak, I. Bratsos, E. Zangrando, J. Kljun, I. Turel, Ž. D. Bugarčić, E. Alessio, *Inorg. Chem.* **2014**, *53* (12), 6113-6126. https://doi.org/10.1021/ic5005215.
[40] M.-C. Pham, M. Oulahyne, M. Mostefai, M. M. Chehimi, *Synth. Met.* **1998**, *93* (2), 89-96. https://doi.org/10.1016/S0379-6779(97)03946-5.
[41] M. Olszowy-Tomczyk, *Chem. Pap.* **2021**, *75* (12), 6157-6167. https://doi.org/10.1007/s11696-021-01799-1.
[42] H. M. A. El-Lateef, T. El-Dabea, M. M. Khalaf, A. M. Abu-Dief, *Antioxidants* **2023**, *12* (2), 213. https://doi.org/10.3390/antiox12020213.
[43] A. A. Adeleke, S. D. Oladipo, R. C. Luckay, E. O. Akintemi, K. A. Olofinsan, I. B. Onajobi, S. T. Yussuf, S. A. Ogundare, O. M. Adeleke, K. I. Babalola, *ChemistrySelect* **2024**, *9* (5). https://doi.org/10.1002/slct.202304967.
[44] R. Ramachandran, P. Viswanathamurthi, *Spectrochim. Acta Part A Mol. Biomol. Spectrosc.* **2013**, *103*, 53-61. https://doi.org/10.1016/j.saa.2012.10.072.
[45] S. Maikoo, A. Chakraborty, N. Vukea, L. M. K. Dingle, W. J. Samson, J.-A. de la Mare, A. L. Edkins, I. N. Booysen, *J. Biomol. Struct. Dyn.* **2021**, *39* (11), 4077-4088. https://doi.org/10.1080/07391102.2020.1775126.
[46] A. V. Oliveira, R. Vilaça, C. N. Santos, V. Costa, R. Menezes, *Biogerontology* **2017**, *18* (1), 3-34. https://doi.org/10.1007/s10522-016-9666-4.
[47] E. Pandur, K. Tamási, R. Pap, E. Varga, A. Miseta, K. Sipos, *Cell. Mol. Neurobiol.* **2019**, *39* (7), 985-1001. https://doi.org/10.1007/s10571-019-00694-4.
[48] K. A. Ahmad, K. B. Iskandar, J. L. Hirpara, M.-V. Clement, S. Pervaiz, *Cancer Res.* **2004**, *64* (21), 7867-7878. https://doi.org/10.1158/0008-5472.CAN-04-0648.
[49] M. H. Asghari, M. Abdollahi, M. R. de Oliveira, S. M. Nabavi, *J. Pharm. Pharmacol.* **2017**, *69* (3), 236-243. https://doi.org/10.1111/jphp.12682.
[50] H. S Kwon, S.-H. Koh, *Transl. Neurodegener.* **2020**, *9* (1), 42. https://doi.org/10.1186/s40035-020-00221-2.
[51] W. Zhang, D. Xiao, Q. Mao, H. Xia, *Signal Transduct. Target. Ther.* **2023**, *8* (1), 267. https://doi.org/10.1038/s41392-023-01486-5.
[52] J. B. Bhagyasree, H. T. Varghese, C. Y. Panicker, J. Samuel, C. Van Alsenoy, K. Bolelli, I. Yildiz, E. Aki, *Spectrochim. Acta Part A Mol. Biomol. Spectrosc.* **2013**, *102*, 99-113. https://doi.org/10.1016/j.saa.2012.09.032.
[53] S. Bonnet, J.-P. Collin, N. Gruber, J.-P. Sauvage, E. R. Schofield, P*Dalt. Trans.* **2003**, No. 24, 4654. https://doi.org/10.1039/b310198c.
[54] L. Conti, G. E. Giacomazzo, B. Valtancoli, M. Perfetti, A. Privitera, C. Giorgi, P. S. Sfragano, I. Palchetti, S. Pecchioli, P. Bruni, F. Cencetti, *Int. J. Mol. Sci.* **2022**. https://doi.org/10.3390/ijms232113302.
[55] Ý. H. Gecibesler, O. Dayan, Z. Şerbetçi, İ. Demirtas, *Pharm. Chem. J.* **2020**, *53* (10), 914-920. https://doi.org/10.1007/s11094-020-02099-w.
[56] S. B. Kedare, R. P. Singh, *J. Food Sci. Technol.* **2011**, *48* (4), 412-422. https://doi.org/10.1007/s13197-011-0251-1.
[57] L. Conti, S. Ciambellotti, G. E. Giacomazzo, V. Ghini, L. Cosottini, E. Puliti, M. Severi, E. Fratini, F. Cencetti, P. Bruni, B. Valtancoli, C. Giorgi, P. Turano, *Inorg. Chem. Front.* **2022**, *9* (6), 1070-1081. https://doi.org/10.1039/D1QI01268A.
[58] M. Verrucchi, G. E. Giacomazzo, P. S. Sfragano, S. Laschi, L. Conti, M. Pagliai, C. Gellini, M. Ricci, E. Ravera, B. Valtancoli, C. Giorgi, I. Palchetti, *Langmuir* **2023**, *39* (1), 679-689. https://doi.org/10.1021/acs.langmuir.2c03042.
[59] D. Maggioni, M. Galli, L. D'Alfonso, D. Inverso, M. V. Dozzi, L. Sironi, M. Iannacone, M. Collini, P. Ferruti, E. Ranucci, G. A. D'Alfonso, L *Inorg. Chem.* **2015**, *54* (2), 544-553. https://doi.org/10.1021/ic502378z.

10.1002/chem.202400834

WILEY VCH

RESEARCH ARTICLE

Entry for the Table of Contents

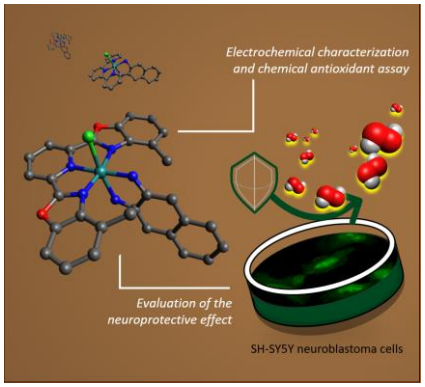

The combination of benzoxazole derivatives with non-innocent ligands in the same ruthenium(II) polypyridyl complex is a suitable strategy to design new pharmacological tools with ROS-scavenging activity against pro-apoptotic/pro-oxidant molecules challenge in human differentiated neuroblasts. The antioxidant properties of such systems are likely the result of a non-trivial synergetic action involving the bioactive ligands in their chemical architectures. The decrease of oxidative stress by these ruthenium(II) systems exerts both pro-survival effect and anti-inflammatory activity in human differentiated neuroblasts.

Institute and/or researcher Twitter usernames: @LucaConti_Chem